Proceedings of Heap Leach Solutions, 2014
November 10–13, 2014, Lima, Peru
Published by InfoMine, © 2014 InfoMine, ISBN: 978-0-9917905-6-2

Secondary recovery of a copper heap leach

Dale F. Rucker, hydroGEOPHYSICS, Inc., USA
Shawn Calendine, hydroGEOPHYSICS, Inc., USA

Abstract

Structural uniformity, that is, the degree to which hydraulic properties are homogenized over space, will affect the degree to which ore is effectively leached. Nonuniform ore has been shown to form preferential flow channels and pooling, and to cause slow drainage, which in turn reduces metal liberation and recovery. In this work, we demonstrate that metal recovery can be increased in a nonuniform and underperforming heap by enhancing the leaching process by directly applying solution to deep areas within the pad. The demonstration was conducted during a pilot-scale test on a copper oxide leach pad, where hydraulic conductivity is low due to a high amount of friable material and high fines content. The ore was then truck dumped and compacted causing serious percolation issues. The demonstration was carried out using four subsurface irrigation (i.e., rinse) wells and nine nearby monitoring wells; the sampling wells were used to extract solution samples for verification. The results showed that: 1) the fine grained ore promoted lateral movement of solution up to 17 m away from the well even at low line pressure; 2) hydraulic conductivity was increased over time by washing the fine grained soil away from material near the well; and 3) additional copper was leached as demonstrated by reduced free acid and high copper concentrations in the sampling wells.

Introduction

Much of the early research in conceptually understanding heap leach processes focused on developing mathematical models to predict ore, solution, gas, and temperature behavior (Roman et al., 1974; Shafer et al., 1979; Letowski, 1980; Bartlett, 1992; Dixon and Hendrix, 1993). From these efforts came large-scale spatiotemporal phenomenological models that can track moisture, metal recovery and remaining inventory, temperature, air movement, and cyanide or free acid consumption (Cross et al., 2006; McBride et al. 2012). More recently, a significant focus has been on improving or optimizing the heap leach process. This focus includes market prices, recovery time, and expenses, balanced with mining constraints as related to heap height, particle size, irrigation rate, curing, and other factors (Padilla et al., 2008). Operationally, Mellado et al. (2011) and Trujillo et al. (2014) examined optimal heap leach design criteria for maximizing a mine's metal recovery and hence income. At a microscale and without considering economics, Petersen and Dixon (2007) optimized zinc recovery by adjusting heap height, irrigation rate, acid concentration, and solution temperature. Other examples of optimized parameterization of leaching processes include Bouffard and West-Sells (2009), Garcia et al. (2010), and Mellado et al. (2010).

Despite all of the best efforts to optimize engineering parameters at the beginning of heap design, there is still a great potential for metal to be left behind after years of leaching. Extracting this last bit of material from the stockpile can be challenging unless the nature of the solution delivery system is drastically changed. As many have discussed, preferential flow of leach solution (e.g., Orr and Vesselinov, 2002; Wu et al., 2007; 2009) will inhibit uniform wetting and drainage through all pore space. These flow channels cannot easily be broken unless there is a significant hydraulic alteration of the pore structure. This can be achieved through pressurized delivery of raffinate via subsurface irrigation as implemented with injection wells (e.g., Seal et al., 2012).

In this paper, we demonstrate the results of a pilot-scale test that used subsurface irrigation on a copper heap leach pad. Subsurface irrigation was implemented using a series of rinse wells. A distinction is made here between injection wells used in previous works and rinse wells, where rinse wells are connected to existing irrigation piping without the use of external booster pumps and apparatus to segregate individual zones along the well. Copper extraction from the leach pad has consistently fallen short of forecasts due to the difficult drainage conditions imposed by fine grained material, and the rinse wells are being used to enhance recovery. It will be shown that based on the ore morphology and grain size distribution, hydraulic alteration can be achieved with rinsing only and that the targeted irrigation method will produce higher copper grades than that reporting to the reclaim (or pregnant leach solution, PLS) pond from surface leaching.

Methodology

Subsurface irrigation can be applied in a number of ways that include adjusting variables associated with application pressure, number of injection zones per well, consideration of extraction wells, drilling method, well casing, and well screening materials. For the injection examples presented for gold mines (Seal et al., 2011, 2012; Winterton and Rucker, 2013), the drilling method was dual rotary that advanced the steel casing during drilling to ensure tight contact with the formation, which minimizes the potential for blowout of the well. The wells were perforated in situ at multiple zones and a high pressure booster pump was employed to maximize the solution coverage for each zone. The high pressure allowed for well placement as far as 35 m from each other using flow rates in excess of 180 m^3/hr and pressures near 20 bar.

In the present application, a hollow stem auger was used for drilling the rinse wells, using PVC casing that was lowered into the hole, and backfill comprising fine-grained material. Since no booster pump was to be used for the experiment, it was thought that the well design would accommodate the lower pressures with no blowout. Additionally, the open hole allowed for monitoring sensors to be placed deep within the heap along the well annulus. The wells had a single application zone at the bottom of the well. At the top of each casing was a valve and a port for monitoring pressure. All wells were plumbed back to an existing irrigation line which had an inline flow meter and totalizer that recorded solution delivery solely to the rinse wells. The monitoring wells were installed in the same manner, but were placed deeper than the rinse wells.

Figure 1 shows the layout of the four rinse and nine monitoring wells. The rinse wells were screened over a 3 m interval, with each well having a different final screened depth between 21 m and 30 m below pad surface. The monitoring wells were screened from 37 m to 46 m. Rinsing was initiated on S1 and continued clockwise around the individual wells. Solution was applied between three to five days per well and only during daytime operating hours. A second test was conducted, where all four rinse wells received solution for a continuous 30 hours.

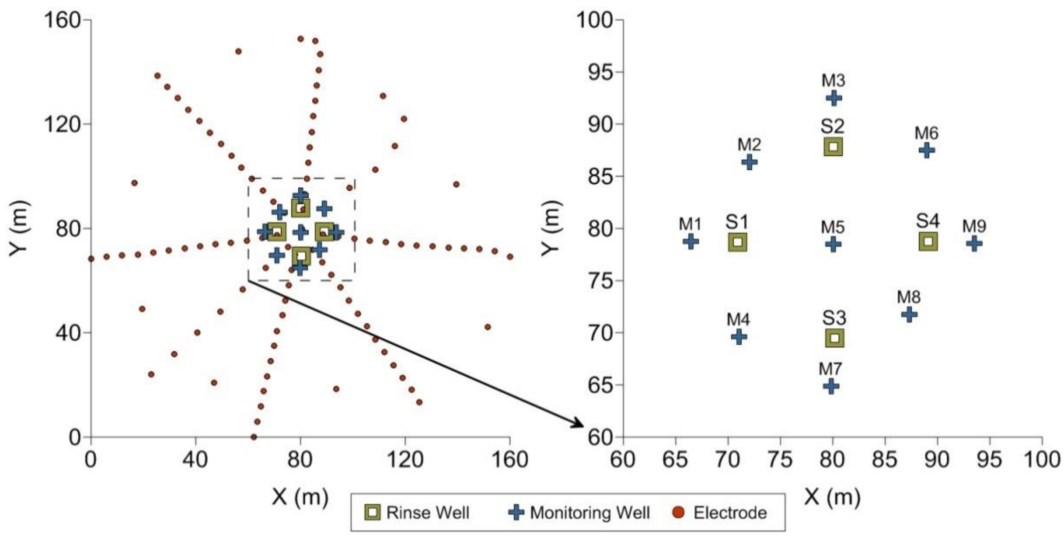

Figure 1: Layout of the rinse and monitoring wells for secondary recovery of copper. Positions of stainless steel electrodes are also shown, which were used to image the solution propagation using electrical resistivity geophysics

Flow and pressure data

Operating objectives were initially developed for the rinsing test that included a minimum flow of 90 m^3/hr with a net copper grade of at least 0.8 g/L averaged over a single eight-hour period. The objectives were developed as a means of recuperating costs associated with drilling, assuming US$6,000 per tonne of copper. In order to verify the flow requirements, gauges were installed that sampled flow rate and pressure at the top of the hole at a sampling interval of 10 s. The high sampling rate allowed for an accurate accounting of raffinate input to the system and for watching material break down and pore structure changes. Table 1 lists the operating parameters during the rinse test on each individual well and the combined rinse using all four wells simultaneously. Figure 2 shows the detailed time series of flow and pressure throughout each test. For the combined rinse, the flow was steady at approximately 337 m^3/hr with pressure at -0.43 bar.

Table 1: Operating hydraulic parameters during the rinse tests on individual and combined wells

Test	Duration (days)	Max. flow (m^3/hr)	Mean flow (m^3/hr)	Total flow (m^3)	Avg. tophole pressure (bar)	Est. bottomhole head (m)
S1	5	180	135	5,150	0.3	24
S2	4	210	146	4,830	1.15	39
S3	5	191	132	4,550	0.23	27
S4	3	208	159	4,090	0.83	39
Combined	1.2	340	337	9,820	−0.43	22

A more detailed hydraulic analysis can be conducted by plotting the flow rate versus pressure and observing how these curves changes over time. Figure 3 presents these data for all four rinse wells. Bottomhole hydraulic head was calculated by adding the tophole pressure to the column of water in the well, without consideration of pipe friction head loss through the screen. The ratio of these two values provides an indication of hydraulic conductivity. In general, the curves show that at the beginning of each rinse period, there is a high head and low flow condition that changes to low head with high flow at the end. These changes are irreversible and permanent, owing to the washout of fine-grained material near the wellbore. The washout creates large pore spaces that result in increased hydraulic conductivity. There are nuances within each test, as in S4 where the last day (Day 2) shows a decrease in hydraulic conductivity. It is hypothesized that the high flows may have washed out a significant amount of material and those voids are filled from material above the zone sometime after the completion of Day 1.

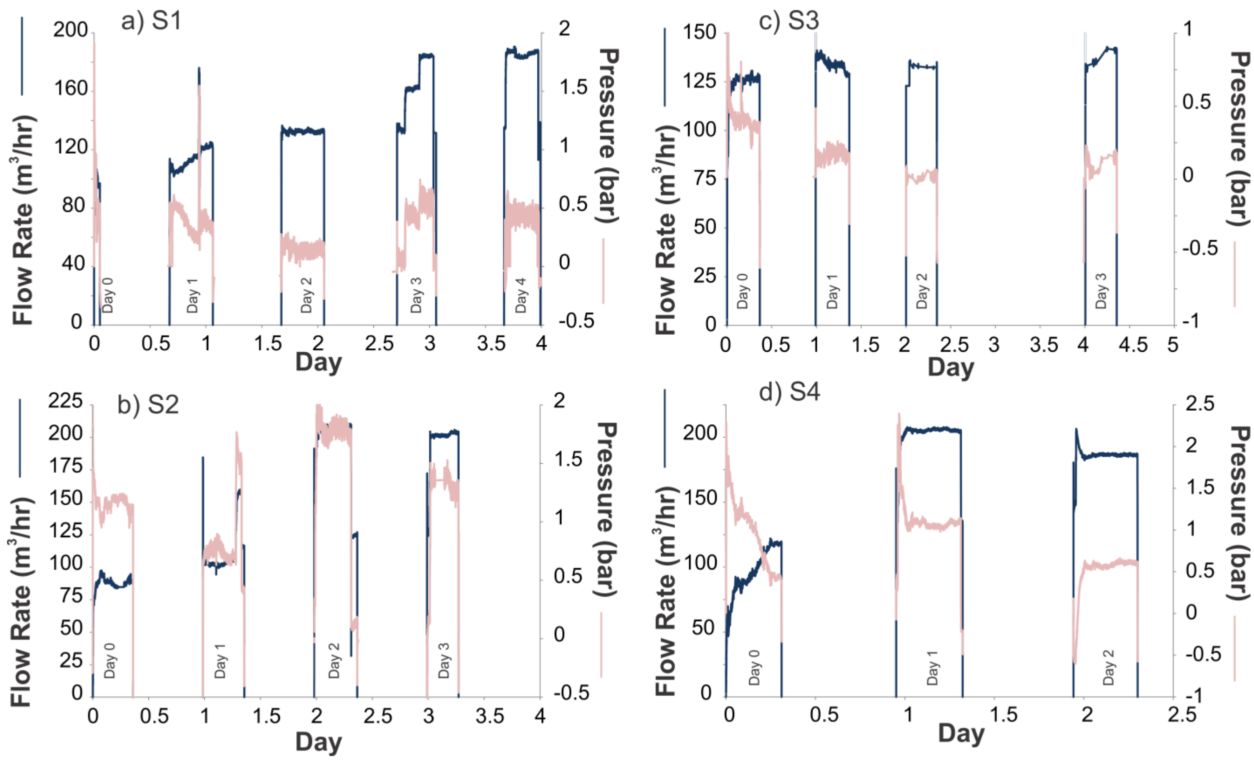

Figure 2: Time series of flow and pressure measured at the wellhead for each rinse test

Solution coverage with geophysical monitoring

The flow of raffinate was monitored using time lapse electrical resistivity geophysics to determine the distance to which the solution travelled. General information about the time lapse electrical resistivity method applied to subsurface injections can be found in Rucker et al. (2009, 2014) and Rucker (2014). For monitoring the rinsing tests, 168 electrodes were distributed along the surface and within the annulus of each well to provide a highly detailed spatiotemporal rendering of the solution propagation. Figure 1 shows the positions of the surface electrodes, where each electrode is constructed of a 1 cm diameter stainless steel rod, approximately 30 cm long. All of the electrodes were wired back to a central acquisition unit, capable of completing a set of measurements (or snapshot) within 25 minutes. Each measurement in a snapshot comprises 167 voltage values while transmitting electrical current on the 168^{th} electrode using a pole-pole array; each electrode has a turn at transmitting current to complete the measurement set. A single snapshot will contain 28,056 data values and each day of monitoring will produce approximately 57 snapshots.

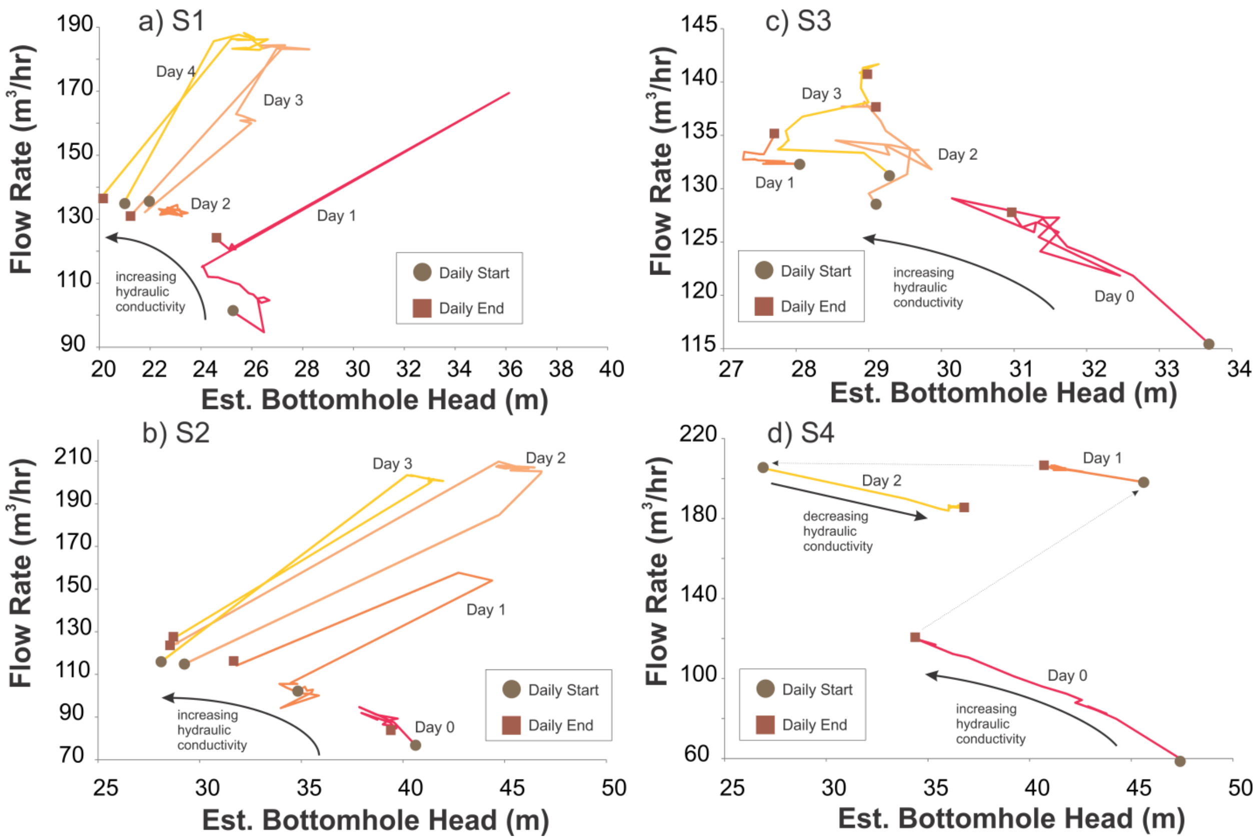

Figure 3: Flow rate versus bottomhole head for each rinse test. The time history from each test provides a qualitative assessment of hydraulic alteration of the pore space

Figure 4 shows solution propagation for the combined well rinse, as interpreted from the geophysical data. For size referencing and positioning, the figure presents two different views for multiple snapshots. The rinse wells and several monitoring wells are placed at the appropriate position and depth. Screens for each well are also shown as larger diameter portions of the well bottom. Lastly, the underliner is shown as color contoured plane with the route the solution would take to the reclaim pond. Directly beneath the well field, the liner was approximately 50 m.

The rendered three-dimensional bodies for the test were developed by calculating a percentage difference for a particular snapshot compared to the baseline prior to the test start. Three bodies are shown in the figure, representing 6% (in red), 12% (in yellow), and 18% (in black) change from baseline. Over the 30 hour test, the solution coverage extends outward from the center of the wellfield to about 24 m. The solution distribution is also asymmetrical with the more intense changes occurring at wells S2 and S4. The other tests conducted on individual wells showed slightly lower coverage, with S1 and S2 radially propagating approximately 17 m. S3 and S4 propagated approximately 12 m from the well center.

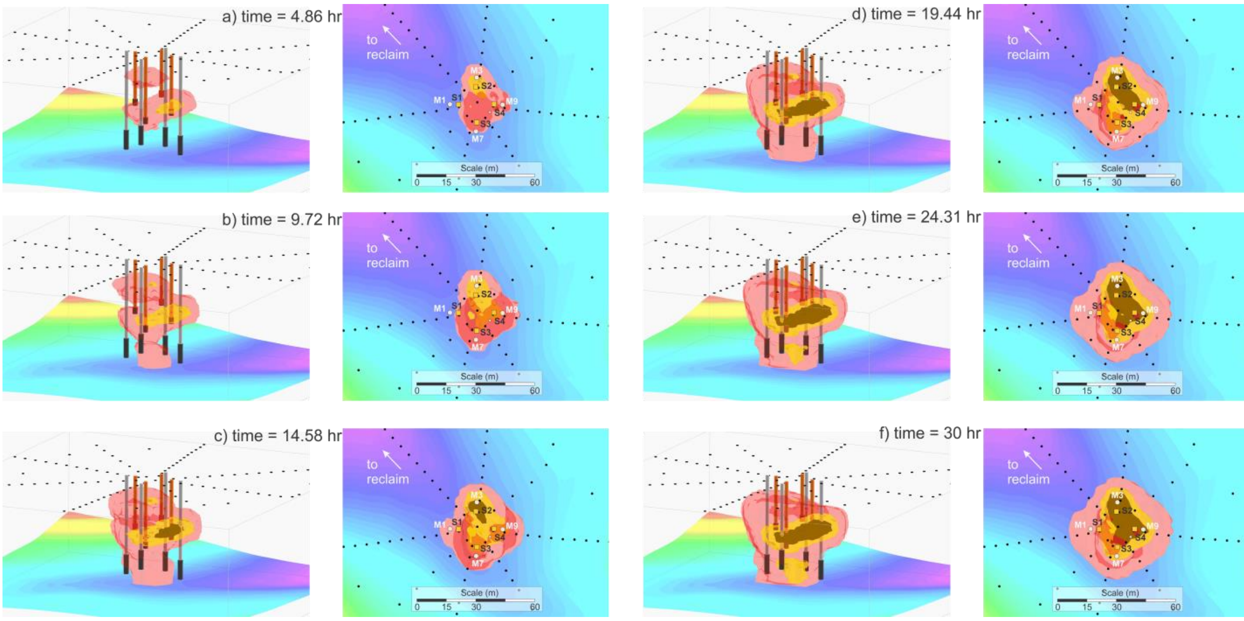

Figure 4: Time lapse electrical resistivity results for the combined well rinse test, showing percent change in resistivity value relative to background. Six evenly distributed snapshots are presented for the 30 hr test. The three rendered bodies represent 6% (red), 12% (yellow), and 18% (black)

Metallurgical monitoring

During the course of the rinsing, samples were withdrawn from the bottom of each monitoring well, two interlift drains located at the edge of the pad (approximately 80 m away), and the raffinate. The sampling rate was higher for those monitoring wells closer to their respective rinse wells, with other wells farther afield sampled less frequently. The sampling procedure included evacuating the well with at least one well volume plus the volume in the hose pump before collecting 1 L of solution for testing. In many cases, several well volumes were purged before testing. The solution sample was split: half stayed locally onsite for testing pH, electrical conductivity, and oxidation-reduction potential (ORP), and the other half went to an analytical lab for a detailed analysis of free acid, copper, iron, and other cations.

Figure 5 shows the results of the simple metallurgical parameters measured onsite, presented as one parameter versus another. The data are segregated among the different monitoring locations and show clear groupings associated with each location. Some wells exhibited high copper recovery whereas others had poor recovery. Moderate recovery (excluding the raffinate) represented those wells and drains that resembled the copper values in the reclaim pond. The monitoring wells with measured high copper recovery generally coincided with rinse wells S1 and S3, which were screened the shallowest at 21 and 24 m, respectively.

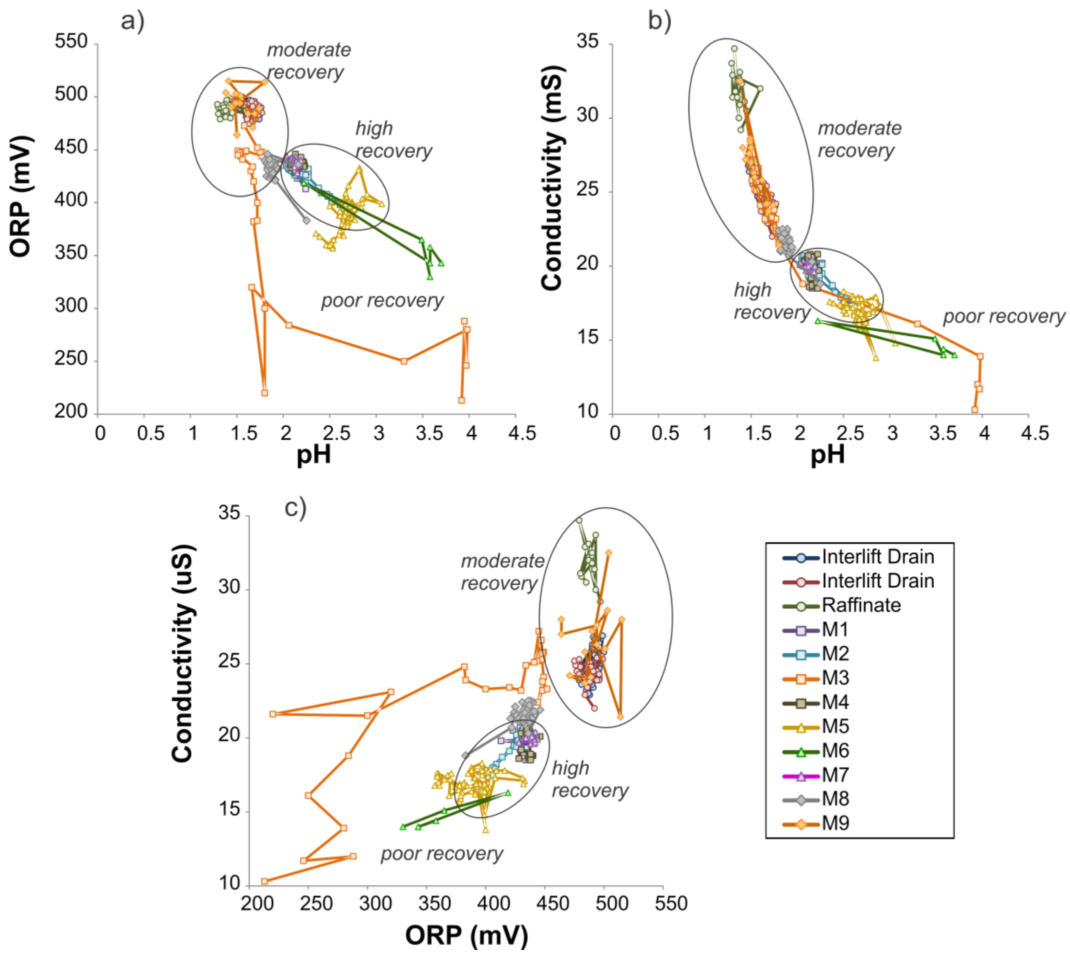

Figure 5: Simple metallurgical parameters acquired from nine monitoring wells, two interlift drains, and raffinate. A) ORP versus pH. B) conductivity versus pH. C) conductivity versus ORP

Time series data showing copper, free acid, and pH are presented in Figure 6. Vertical gray bars distinguish each rinsing period. The qualitative recovery determination from Figure 5 was taken from the copper data of Figure 6. Monitoring wells M1, M2, M4, M5, and M7 consistently show copper above 2 g/L. During rinsing on S2, well M2 briefly nears 4 g/L copper, which also corresponded to a decrease in free acid and increase in pH. Monitoring well M8 dropped over time to about 1.5 g/L. Moderate recovery, where values were near 1 g/L, included the interlift drains and M9.

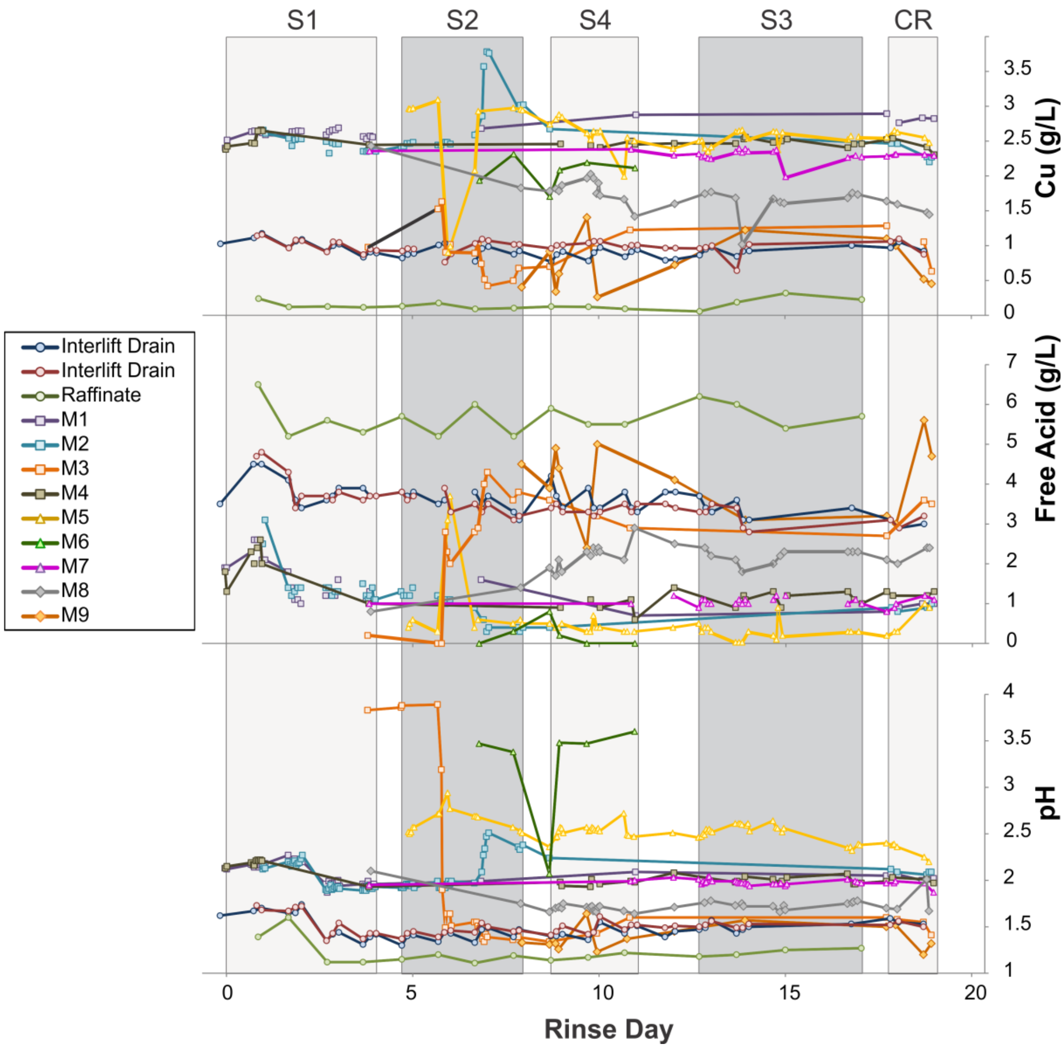

Figure 6: Time series of analytical chemistry data from different monitoring locations during the five rinsing phases, including copper, free acid, and pH. CR = combined rinse

Integrating the average net copper grade (total measured copper minus raffinate copper grade) for each rinse test and multiplying by total solution delivery yielded approximately 52,800 kg of copper liberated during this pilot-scale test. The rinse test lasted 20 days. The largest contribution came from the combined rinse, where average copper grade from all nine monitoring wells was 1.75 g/L. The smallest contribution came from well S4 (average grade of 1.48 g/L), where hydraulic conditions and solution delivery were not optimized for extraction. The first rinse on S1 showed the largest average net copper grade at 2.23 g/L.

Conclusion

A pilot-scale subsurface irrigation test to enhance the recovery of copper was demonstrated on a copper oxide heap. The test was designed with four rinse wells, which received solution directly from an irrigation line without the use of onsite booster pumps that have been described in other works (e.g., Seal et al., 2012). Flows to the well ranged from about 130 to 330 m^3/hr.

A large effort was expended to validate the effectiveness of the method and ensure that initial test objectives were met. The test objectives were designed to offset drilling costs and included a minimum flow of 90 m^3/hr and a time weighted average of 0.8 g/L copper in the pregnant solution sustained for at least eight hours. The validation measures included a number of monitoring technologies that measured in situ hydraulic properties and ex situ water chemistry data. Hydraulic properties were measured with flow and pressure gauges and the data were recorded at a high sampling rate. Time lapse electrical resistivity geophysics was also used to track the movement of the pregnant solution. To obtain solution samples, monitoring wells were installed near the rinse wells and samples were withdrawn at sampling rates between one and three hours.

By all measures, the pilot enhanced recovery test was a success. Maximum flow rates were at least double the objective and the mean flow rate was about 1.5 times the objective. The high flow rate also provided a means to washout the fine grained material near the wellbore and expose new surfaces to the raffinate. The copper grades exceeded the test objective by a factor of three in many cases and upwards to a factor of five for a short period in a single monitoring well. Additionally, the high grades were sustained longer than anticipated. Actual leaching was confirmed by the lowered free acid, which was significantly lower than those samples that represented surface irrigation. In fact, it appears that the acid consumption is about three times greater during rinsing than surface irrigation, which could be attributed to the greater surface area exposed during the hydraulic alteration of the pore space and fluidization of small particles.

Lastly, electrical resistivity geophysics was conducted to observe volumetric changes to the formation during rinsing. The resistivity parameter is sensitive to a number of phenomena occurring simultaneously, including saturation, porosity, and solution conductivity. The time lapse models showed a low resistivity body increasing outward from the well screen. The final position of the body at the end of each individual rinse test was used to infer the lateral solution coverage. Excluding the combined rinse, solution coverage was shown to be the largest in S1 and S2 (radial distance of approximately 17 m from the well center) when flow rates were gradually increased over a few days. In contrast, the rinse on S4 allowed high flow rates from the beginning, with a radial coverage of about 12 m. The high flow rates likely carried all fine grained material at once to an outer shell, which may have sealed off the formation and limited solution coverage.

References

Bartlett, R.W. 1992. "Simulation of Ore Heap Leaching Using Deterministic Models," Hydrometallurgy, 29: 231–260.

Bouffard, S.C. and West-Sells, P.G. 2009. "Hydrodynamic Behavior of Heap Leach Piles: Influence of Testing Scale and Material Properties," Hydrometallurgy, 98: 136–142.

Cross, M., Bennett, C.R., Croft, T.N., McBride, D., and Gebhardt, J.E. 2006. "Computational Modelling of Reactive Multi-Phase Flows in Porous Media: Applications to Metals Extraction And Environmental Recovery Processes," Minerals Engineering, 19: 1098–1108.

Dixon, D.G. and Hendrix, J.L. 1993. "A General Model for Leaching of One or More Solid Reactants from Porous Ore Particles," Metallurgical Transactions B, 24B: 157-169.

Garcia, S., Ramon, C., Esplin, A., Gebhardt, J.E., Hernandez, A., McBride, D., and Cross, M. 2010. "Gold Heap Leach Simulation and Optimization Using a Multiphysics Model," Minerals and Metallurgical Processing, 27: 196–204.

Letowski, F. 1980. "Ore Leaching Model with Partial Decomposition of Rocks. I. Theoretical Predictions," Hydrometallurgy, 6: 121–133.

McBride, D., Gebhardt, J.E., and Cross, M. 2012. "A Comprehensive Gold Oxide Heap Leach Model: Development and Validation," Hydrometallurgy, 113–114: 98–108.

Mellado, M.E., Gálvez, E.D., and Cisternas, L.A. 2010. "On the Optimization of Flow Rates on Copper Heap Leaching Operations," International Journal of Mineral Processing, 101: 75–80

Mellado, M.E., Casanova, M.P., Cisternas, L.A., and Gálvez, E.D. 2011. "On Scalable Analytical Models for Heap Leaching," Computers and Chemical Engineering, 35: 220–225.

Orr, S. and Vesselinov, V. 2002. "Enhanced Heap Leaching — Part 2: Applications," Mining Engineering, 54 (10): 33–38.

Padilla, G.A., Cisternas, L.A., and Cueto, J.Y. 2008. "On the Optimization of Heap Leaching," Minerals Engineering, 21: 673–678.

Petersen, J. and Dixon, D.G. 2007. "Modelling Zinc Heap Bioleaching," Hydrometallurgy, 85: 127–143.

Roman, R.J., Benner B.R., and Becker, G.W. 1974. "Diffusion Model for Heap Leaching and its Application to Scale-Up," SME Transactions, 256: 247-252.

Rucker, D.F. 2014. "Investigating Motion Blur and Temporal Aliasing from Time-Lapse Electrical Resistivity," Journal of Applied Geophysics, (in press).

Rucker, D.F., McNeill, M., Schindler, A., and Noonan, G.E. 2009. "Monitoring of a Secondary Recovery Application of Leachate Injection into a Heap," Hydrometallurgy, 99: 238-248.

Rucker, D.F., Crook, N., Winterton, J., McNeill, M., Baldyga, C.A., Noonan, G., and Fink, J.B. 2014. "Real-Time Electrical Monitoring of Reagent Delivery during a Subsurface Amendment Experiment," Near Surface Geophysics, 12: 151-163.

Seal, T., Winterton, J., and Rucker, D.F. 2011. "Hydro-Jex Monitoring and Operations at the Cripple Creek and Victor Heap Leach Operation in Colorado, USA," Proceedings of Society of Mining Metallurgical and Exploration Annual Meeting, Phoenix, AZ. SME

Seal, T., Rucker, D.F., and Winterton, J. 2012. "Enhancing Gold Recovery Using Hydro-Je at Cripple Creek and Victor Gold Mine Co." in Separation Technologies for Minerals, Coal & Earth Resources, (eds C.A. Young and G.H. Luttrell). Society for Mining, Metallurgy, and Exploration, Denver.

Shafer, J.L., White, M.L., and Caenepeel, C.L. 1979. "Application of the Shrinking Core Model for Copper Oxide Leaching," Mining Engineering, 31: 165 – 171.

Trujillo, J.Y., Cisternas, L.A., Gálvez, E.D., and Mellado, M.E. 2014. "Optimal Design and Planning of Heap Leaching Process. Application to copper oxide leaching," Chemical Engineering Research and Design, 92: 308-317.

Winterton, J. and Rucker, D.F. 2013. "Optimal Strategies for Leach Pad Injection Operations," Proceedings of the Society of Mining Metallurgical and Exploration Annual Meeting, Denver, CO. SME

Wu, A., Yin, S., Yang, B., Wang, J., and Qiu, G. 2007. "Study on Preferential Flow in Dump Leaching of Low-Grade Ores," Hydrometallurgy, 87: 124–132.

Wu, A., Yin, S., Qin, W., Liu, J., and Qiu, G. 2009. "The Effect of Preferential Flow on Extraction and Surface Morphology of Copper Sulphides during Heap Leaching," Hydrometallurgy, 95: 76–81.